ALLOSOURCE

THE BIOMECHANICS AND BIOLOGICAL PROPERTIES OF ALLOMEND® ACELLULAR DERMAL MATRIX: A SUMMARY

AlloSource®, Centennial, CO

The Biomechanics and Biological Properties of AlloMend® Acellular Dermal Matrix: A Summary

AlloSource®, Centennial, CO

INTRODUCTION

Acellular dermal matrices (ADMs) can be successfully used to replace or repair integumental soft tissue compromised by disease, injury or surgical procedures. These biomaterials are used surgically for a wide range of regenerative and reconstructive medicine applications, including abdominal wall reconstruction/hernia repair, breast reconstruction, tendon augmentation, superior capsular reconstruction and pelvic organ prolapse repair, among others.[1,2,3,4,5,6,7,8]

In this presentation, we summarize the internal findings regarding AlloMend® ADM acellular human dermal matrix tissue (AlloSource®, Centennial, CO) for five significant properties that help determine the suitability of an ADM for use in these and other applications. The complete reports (*Figure 1*) with additional details on the testing protocols underlying these findings are available from AlloSource.

- Biocompatibility – AlloMend ADM's evidence of tissue incorporation and vascularization was documented in animal studies.[9]
- Growth factors – AlloMend ADM maintained four primary growth proteins when analyzed in ELISA testing.[10]
- Tensile strength – AlloMend ADM exhibited an ultimate tensile strength (UTS) of 20.7 MPa ± 2.2, surpassing published UTS data for other leading ADM products.[11]
- Suture retention strength – AlloMend ADM withstood pulling tension equivalent to the force that a 2-0 suture would be expected to withstand.[12]
- Fluid egress and surface area – AlloMend ADM in a meshed configuration demonstrated significant fluid egress and surface area coverage.[13]

Figure 1. *Series of Five AlloMend ADM Biomechanics Analyses.*

Processing

AlloMend ADM (*Figure 2*), is an acellular human dermal matrix tissue processed through AlloSource's proprietary DermaTrue™ decellularization process. This process disrupts cells and removes cellular debris (including DNA, RNA, proteins and antigens), rendering the tissue biocompatible. Further, the tissue has been tested by standard ISO 10993-5 methodology and was found to be non-cytotoxic.

DermaTrue does not use detergents or enzymes, leaving no harmful residuals in the tissue, while retaining native growth factors and the morphological collagen-elastic structure. As the decellularization process also inactivates microorganisms, as a result, the likelihood of inflammation or immunogenic rejection response by the recipient is further minimized.

The tissue undergoes a terminal e-beam sterilization procedure, resulting in a 10^{-6} Sterility Assurance Level (SAL), meeting the same stringent sterility levels required by the U.S. Food and Drug Administration for implantable biomedical devices. Because of its terminal sterilization, AlloMend ADM can be stored at room temperature for up to two years.

Unlike some other acellular dermal matrices, the tissue is pre-hydrated and ready for immediate use without requiring a lengthy rehydration period. In addition, due to its elasticity and suppleness, AlloMend ADM can be easily placed in a variety of anatomical areas.

Figure 2. *AlloMend ADM Tissue.*

Biocompatibility

In an *in vivo* tissue graft environment, biocompatibility results in the incorporation of the implanted graft into the host tissue to the point where there is no discernible difference between the two in form and function.

A standard *in vivo* study was conducted in which 12 rats were implanted subcutaneously with sections of AlloMend ADM from four different donors (*Figure 3)*. A doctor of veterinary medicine monitored the animals' well-being and conducted the clinical assessments of the animals following the implantation procedures.

The animals were sacrificed at three time intervals: two weeks, six weeks and twelve weeks post-implementation. After euthanasia, the implants (*Figure 4*) were removed and submitted to a board-certified veterinary pathologist for a histological assessment of the integrity of the implant and the infiltration of blood vessels into the graft. Standard, documented procedures[14,15] were used in the assessment.

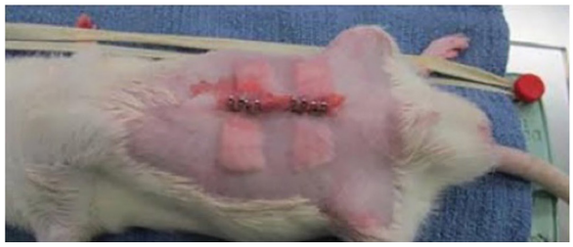

Figure 3. *Initial implant of AlloMend ADM at time 0.*

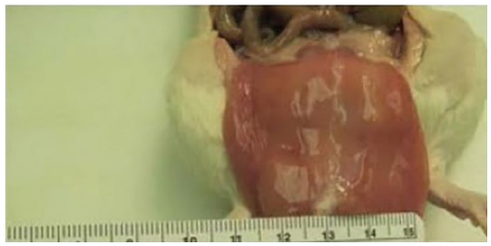

Figure 4. *Implanted AlloMend ADM at 14 days.*

Two days after implantation procedures, visible swelling and erythema were resolved normally, an initial indication of graft incorporation. Similarly, all of the animals gained weight at rates consistent with normal rats, evidence that the grafts did not inhibit metabolic growth. At the time of explantation, all of the animals were deemed healthy by the veterinarian, suggesting there was no significant immunogenic response to the graft.

Upon necropsy, all animals were determined to have developed normally during the period and no untoward tissue rejection was apparent. Histological examination of the explanted tissue indicated cell and vessel infiltration for all three time periods (*Figures 5 and 6*). No significant levels of graft encapsulation were observed, indicating the absence of inflammatory response tissue rejection.

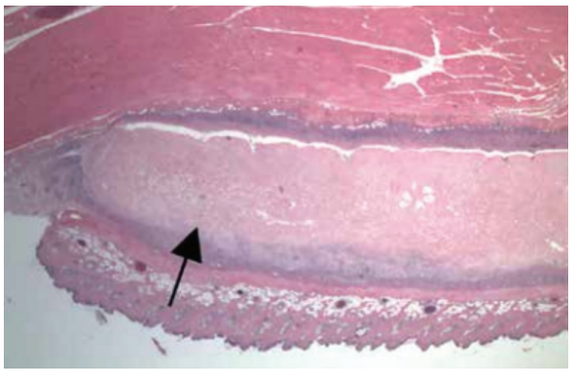

Figure 5. *Graft implantation (arrow) at two weeks.*

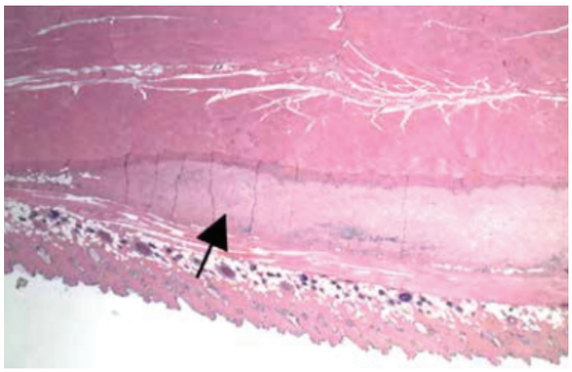

Figure 6. *Graft implantation (arrow) at 12 weeks.*

Vascularization was confirmed through immunohistochemistry staining (*Figure 7*) for the presence of von Willebrand Factor (vWF), a key component of the blood clotting cascade and a reliable marker protein for endothelial cells of blood vessels.[16]

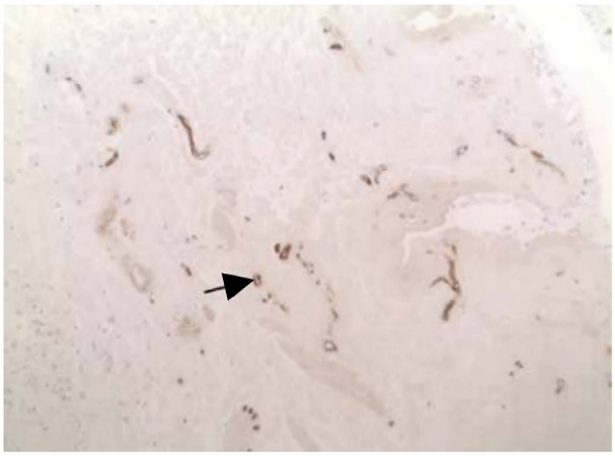

Figure 7. *Immunohistochemistry staining for von Willebrand Factor in an AlloMend graft at six weeks. Arrow indicates a blood vessel.*

Finally, even though AlloMend ADM was implanted without suturing and no encapsulation was found, the grafts stayed in place with very little evidence of migration, suggesting there was incorporation of AlloMend ADM.

In summary, there was strong evidence of tissue incorporation and blood vessel infiltration. No encapsulation or infections were noted. There was no discernible impact on metabolism – animal growth and development subsequent to implantation were normal.

Growth Factors

The presence of growth factors in an implanted ADM can stimulate healing and revascularization, as well as inhibit scarring[17,18] in a variety of procedures, including soft tissue repair. In these applications the use of a graft containing growth factors helps promote scar-free healing and proper graft incorporation without allogeneic rejection. AlloSource researchers tested AlloMend ADM for the presence of four specific growth factors. These have been extensively studied by researchers, and are widely known to contribute to a healing response:

- Fibroblast Growth Factor (bFGF)[19,20,21,22,23,24,25,26]
- Platelet Derived Growth Factor (PDGFbb)[27,28,29,30,31]
- Transforming Growth Factor (TGFb)[32,33,34,35,36,37,38]
- Bone Morphogenic Protein 2 (BMP2)[39,40,41,42]

The role each of these proteins plays in a range of procedures is summarized in *Table 1.*

	Soft Tissue Reconstruction	Total Surgical Site Benefits
bFGF	Assists in angiogenesis basal membrane formation Prevents necrosis	Prevents necrosis Promotes scar-free healing Promotes surgical wound closure
PDGFbb	Reduces inflammation Serves as a chemotactic guide to graft for host cells	Promotes scar-free healing
TGFb	Assists in the production of new matrix in graft Promotes allograft acceptance	Prevents inflammation Coordinates the wound healing process
BMP2	Serves as a chemotactic guide to graft for host cells Induces adipogenesis in soft tissue spaces	Promotes stem cell differentiation

Table 1. *Significance of growth factors in allograft procedures.*

This growth factor assay utilized AlloMend ADM tissues from four donors. The grafts were cut into 1.0 mm square cubes and homogenized in Raybiotech Lysis buffer. Thermo Scientific Halt Protease Inhibitor cocktail was added. The process utilized a VWR VDI 25 Homogenizer and the homogenate was kept on ice for 30 minutes and sonicated for two minutes. The homogenates were centrifuged at 12,000 G for 10 minutes and the supernatant was collected and stored at -80° C until use.

The tissue homogenate was analyzed using ELISA sandwich kits (RayBiotech, Atlanta, GA) to detect BMP2, bFGF and PDGFbb as illustrated in *Figure 8*. An additional ELISA kit (Enzo Biochem, Farmington, NY) was used to detect TGFb.

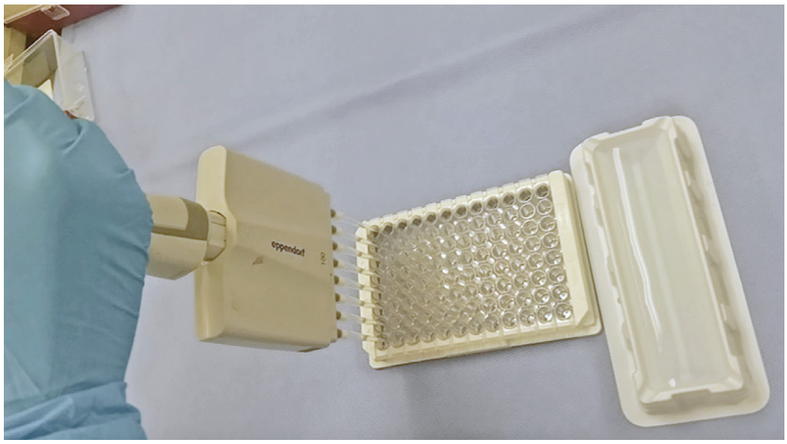

Figure 8. *Pipetting process during ELISA analysis of AlloMend ADM.*

The ELISA testing revealed the presence of BMP2, PDGFbb and bFGF in all four of the grafts. TGFb was found in three of the four grafts.

Tensile Strength

The ultimate tensile strength (UTS) of a biomaterial is the maximum stress or strain it can withstand while being stretched or pulled to the point of breaking or failing.

Fully processed and sterilized AlloMend ADM samples were tested in an electro-mechanical device designed for measuring and recording the stress-strain characteristics of biomaterials (*Figure 9*). Samples were cut and tested by a protocol outlining acceptable methodologies for UTS similar to those laid out in USP's Bovine Dermal Matrix (tensile test)[43] and ASTM's Standard Test Method for Tensile Properties of Plastics.[44]

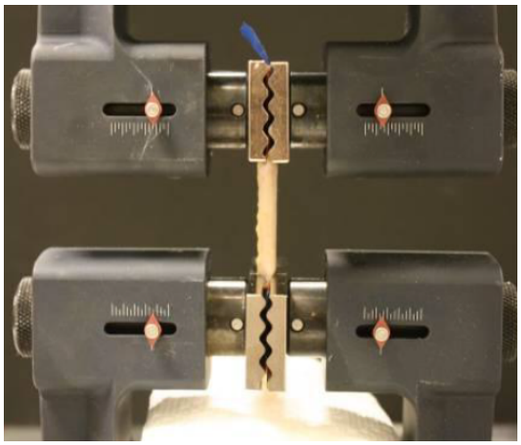

Figure 9. *Static Tension Grip Fixture.*

A tensile load was applied to each specimen using an electro-mechanical test machine at a rate of 10mm per minute under displacement control until failure was achieved. Failure was designated as a rapid loss in tensile force with compromised tissue. The force required to cause failure was recorded as UTS.

AlloMend ADM exhibited UTS of 20.7 MPa ± 2.2, many times stronger than intra-abdominal pressure maximums, surpassing published UTS data for other leading acellular dermal matrix products (*Figure 10*).

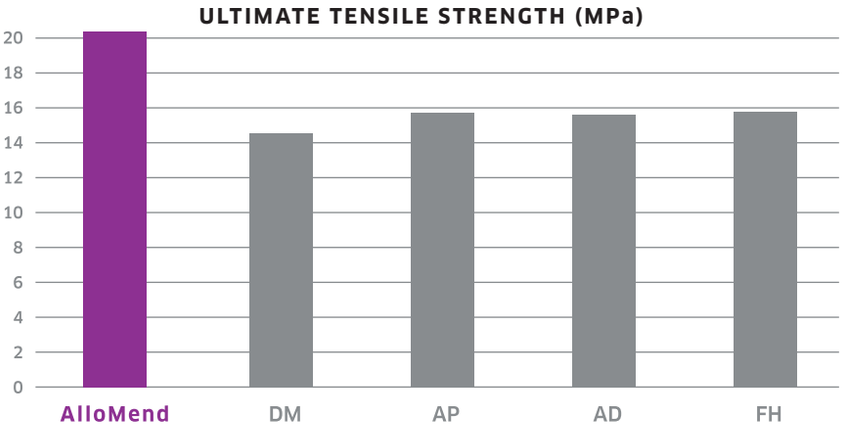

Figure 10. *Ultimate Tensile Strength (MPa) Comparison of Dermal Matrix Products Based on Published Data on File at AlloSource.*

DM is DermaMatrix Acellular Dermis (Synthes)
AP is AlloPatch HD Acellular Human Dermis (MTF)
AD is AlloDerm Freeze-Dried Acellular Dermal Matrix Graft (LifeCell)
FH is FlexHD Acellular Hydrated Dermis (Ethicon)

Suture Retention

Suture retention strength is the maximum pulling force measured in Newtons (N) on a suture that a tissue can bear at the point of suture before the suture tears through the tissue.

AlloMend ADM grafts from seven different donors (41 samples total) were used in the study. They were prepared in a range of thicknesses from 1.29 to 4.05 mm and cut into approximately 4.0 x 4.0 cm pieces.

All testing was performed using a MTS Model 820.050-SL or ADMET 2600 uniaxial testing apparatus (MTS Systems Corporation, Eden Prairie, MN, or ADMET, Norwich, CT) in accordance with accepted practices for measuring ultimate suture retention strength.[45,46]

In each case, the tissue was secured in the testing apparatus with 2.0 cm of hanging tissue remaining (*Figure 11*). A simple loop of Anthrex FiberWire 2/metric 5 suture was placed through the tissue approximately 1.0 cm from the edge. This particular suture is one of the strongest available and thus it was used in this test to ensure there would be no suture failure except if exposed to the most extreme forces.

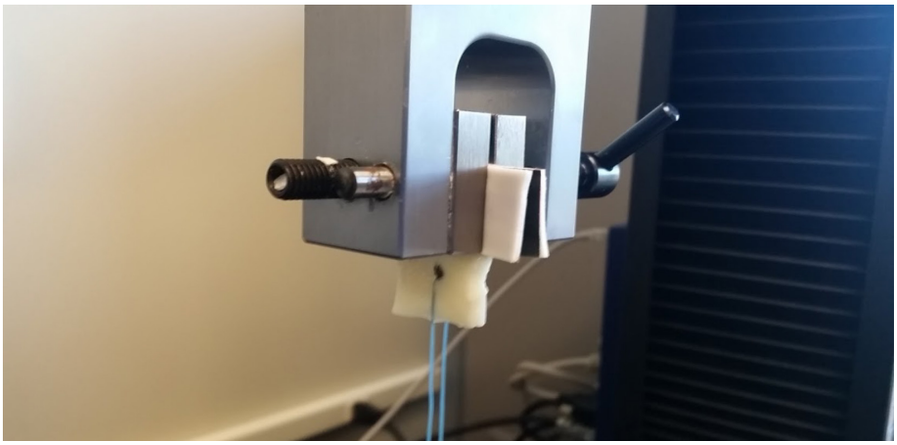

Figure 11. *AlloMend Tissue Secured to ADMET Machine with Suture – Pretesting.*

A tension test was executed at 20.0 mm/min until the point of complete suture pullout. The maximum load on the tissue just prior to suture pullout was recorded for each sample.

As would be expected, the suture pullout strength for each sample was closely correlated to the thickness of the AlloMend ADM graft, as demonstrated in *Figure 12.*

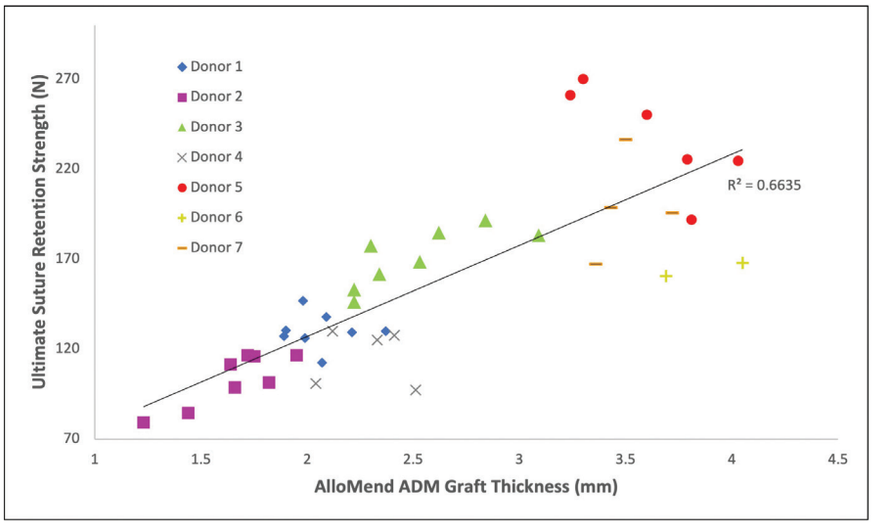

Figure 12. *Relation between Graft Thickness and Suture Pullout.*

An analysis of suture pullout strength per unit of thickness yielded a mean value of 61.4 N/mm. The most commonly used AlloMend ADM products are from the AlloMend T configuration (from 1.0–2.0 mm).

Therefore, depending on their precise thicknesses, the tissue grafts in this range can be expected to have an ultimate suture pullout strength of between 61 and 123 N. The thickest graft, AlloMend UT (from 3.0–4.0 mm), extended the range up to 161 to 270 N.

Fluid Egress and Surface Area

Meshing (cutting slits) or perforating (stamping small holes) the graft allows fluid to flow through it (egress). Enhanced fluid egress can reduce the risk of seroma, which can slow vascular ingrowth and postpone integration of the graft,[47] the most common complication reported in breast reconstructions using ADM tissue.[48] These modifications also can enhance conformability and increase the surface area of the ADM graft that remains in contact with the wound bed, possibly allowing for more rapid vascularization and faster patient recovery.[22]

AlloSource compared the fluid egress properties and respective surface areas of perforated and meshed ADM tissue. The study utilized three different cut patterns for ADM tissues. The first (Perforated #1) is representative of a commercially available graft. The second (Perforated #2) approximately doubles the perforation density of Perforation #1). The third (Meshed) incorporates 130 mesh lines, 1.5 mm long in a 2x2 cm graft (*Figure 13*).

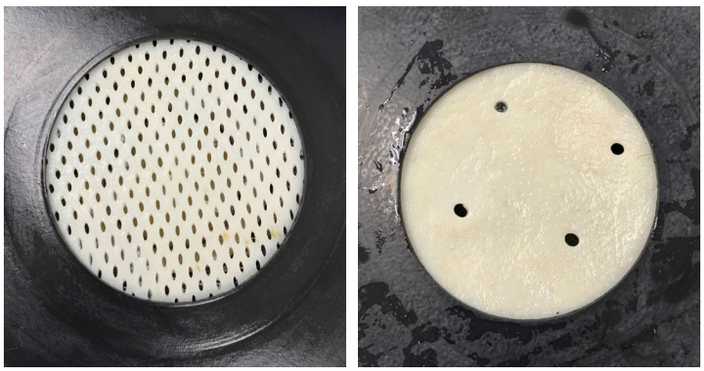

Figure 13. *Representative photos of Meshed (left) and Perforated Pattern #1 (right) placed in the fluid egress testing device.*

Analyzing Fluid Egress

Six full thickness ADM tissues from three different donors were processed. From each donor, two samples of each of the three cut patterns were prepared. Thus, the study utilized 18 total samples, six of each cut pattern. Sample thickness was measured in five locations and recorded.

AlloSource researchers designed a testing device (*Figure 14*) to measure the fluid egress properties of the 18 tissues. The ADM samples were placed between two pipe flanges with a valve below and clear pipe above. The pipe was filled with fetal bovine serum (FBS). The valve was opened, allowing fluid to flow through the sample. A camera recorded the amount of time required for the FBS to pass between two lines on the pipe (21.6 cm). Each sample was run in triplicate.

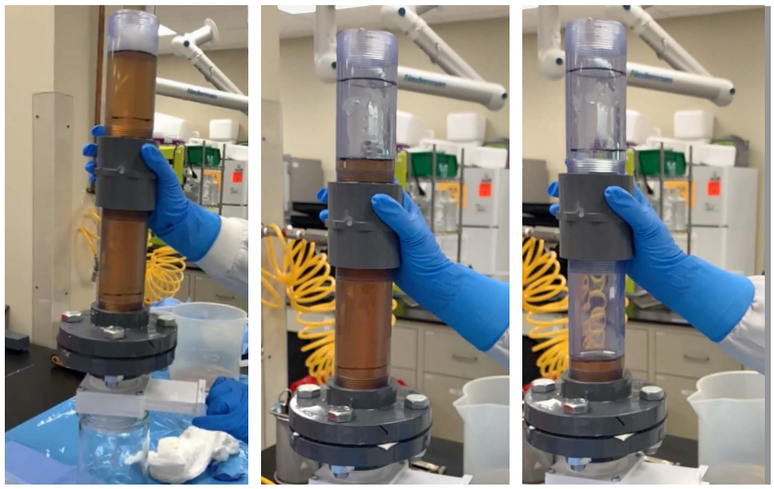

Figure 14. *Fluid egress testing device. The pipe was filled to the fill line (left) with FBS and the time was recorded as it passed from Line 1 (middle) to Line 2 (right) for each sample.*

The time required for fluid to pass from line 1 to line 2 of the fluid egress testing device was recorded for each sample in triplicate. The average egress time for each variety of cut tissue was calculated. As seen in *Table 2*, there was a significant difference in egress properties across the three patterns (Minitab 17, One-Way ANOVA, p=0.000).

PATTERN	AVERAGE TIME	STANDARD DEVIATION	95% CONFIDENCE INTERVAL
Perforated 1	10.369 seconds	1.598 seconds	(9.189, 11.549)
Perforated 2	6.504 seconds	1.273 seconds	(5.324, 7.683)
Meshed	1.974 seconds	1.157 seconds	(0.795, 3.154)

Table 2. *Draining Times for Meshed and Perforated ADM.*

In the study, the Meshed ADM tissue had an average volumetric flow rate approximately 5.3 times that of the Perforated Pattern #1 tissue and approximately 3.3 times the flow rate of the Perforated Pattern #2 tissue. Thus, a meshed ADM would seem to significantly improve the fluid egress properties of the graft compared to perforated tissue at either of the two tested perforation densities.

A General Linear Model ANOVA indicated that neither donor (p=0.249) nor graft thickness (p=0.914) had a significant impact on the results.

Analyzing Surface Area

Meshing or perforating ADM tissue can change its surface area due to the additional area inside the pores. The surface area of these modified ADM samples is calculated based on the length, width and thickness of the graft, as well as accounting for the mesh length or the perforation diameter. SolidWorks was used to visualize each of the three patterns. The tissue thickness was assumed to be 1 mm for purpose of this analysis.

Meshed Sample

Unlike the perforating process, meshing does not remove any material from the graft. Instead, small lines are cut into the tissue and as the graft is stretched, each line becomes a small pore. Thus, the surface area of a meshed graft is equal to the entire surface area of the top of the graft plus the area inside of the pores. The calculation for the surface area of a meshed tissue is as follows:

$$\textit{Surface Area} = (\textit{Original Area}) + (\#\ \textit{mesh lines}) * (\textit{perimeter of mesh hole}) * (\textit{graft thickness})$$

$$\textit{Surface Area} = (4\ cm^2) + (130)(2 * 1.5\ mm)(1\ mm)$$

$$\textit{Surface Area} = 4\ cm^2 + 3.9\ cm^2 = 7.9\ cm^2$$

$$\textbf{Increase in Surface Area from Meshing} = \frac{7.9 - 4}{4} * 100\% = 97.5\%$$

Thus, meshing in a 1:1 pattern nearly doubles the surface area of the graft.

Perforated Samples

The 2-dimensional surface area of a perforated ADM graft is reduced when holes are stamped into it, but at the same time, the 3-dimensional surface area is increased by the area inside the hole. In a 16x20 cm graft, the area of a perforated surface for each sample is calculated as follows:

PERFORATED PATTERN #1

$$\textit{Surface Area} = (\textit{2-dimensional, area of top of graft}) + (\#\ \textit{holes}) * (\textit{area of inside of hole})$$

$$\textit{Surface Area} = 317.1018\ cm^2 + (41\ \textit{holes})(0.09424\ cm^2)$$

$$\textit{Surface Area} = 320.966\ cm^2$$

$$\textit{Original Graft Area} = (16\ cm)(20\ cm) = 320\ cm^2$$

$$\textbf{Increase in Surface Area from Perforation Pattern \#1} = \frac{320.966 - 320}{320} * 100\% = 0.3\%$$

PERFORATED PATTERN #2

Surface Area = (area of top of graft) + (# holes) * (area of inside of hole)

Surface Area = 314.34513 cm^2 + (80)(0.09424 cm^2)

Surface Area = 321.884 cm^2

Original Graft Area = (16 cm)(20 cm) = 320 cm^2

$$\textbf{Increase in Surface Area from Perforation Pattern \#1} = \frac{321.884 - 320}{320} * 100\% = 0.59\%$$

Thus, compared to an unmodified ADM tissue sheet, perforation at these two densities yielded less than a one percent increase in the surface area of the ADM tissue. In contrast, meshing the tissue nearly doubled its surface area.

CONCLUSION

AlloMend ADM can meet and exceed all surgical requirements in terms of secure placement in the course of soft tissue repair. It introduces essential growth factors to the wound site, and its biocompatibility with surrounding tissue helps ensure incorporation. It offers high suture retention and tensile strength while retaining essential flexibility and pliability characteristics allowing for secure placement and suturing. The meshed AlloMend ADM further allows fluid egress while increasing surface area contact. These attributes, along with its assured terminal sterility, room temperature storage, pre-hydrated format and the DermaTrue Decellularization Process make AlloMend ADM an ideal extracellular dermal matrix tissue for a wide range of tissue reconstruction applications.

References

1. Peppas G, et al. Biological mesh in hernia repair, abdominal wall defects, and reconstruction and treatment of pelvic organ prolapse: A review of the clinical evidence. *Am Surg*. 2010; 76(11):1290–9.
2. Macadam SA, et al. Acellular dermal matrices: Use in reconstructive and aesthetic breast surgery. *Can J Plast Surg*. 2012; 20(2):75–89.
3. Griffin TJ, et al. Hard and soft tissue augmentation in implant therapy using acellular dermal matrix. *Int J Periodontics Restorative Dent*. 2004; 24(4):352–61.
4. Costantino PD, et al. Acellular dermis for facial soft tissue augmentation: Preliminary report. *Arch Facial Plast Surg*. 2001; 3(1):38–43.
5. Rapley JH, et al. Mid-substance peroneal tendon defects augmented with an acellular dermal matrix allograft. *Foot Ankle Int*. 2010; 31(2):136–40.
6. Barber FA, et al. A prospective, randomized evaluation of acellular human dermal matrix augmentation for arthroscopic rotator cuff repair. *Arthroscopy*. 2012; 28(1):8–15.
7. Frisella, A. Superior capsular reconstruction with AlloMend acellular dermal matrix for reconstruction of a massive, irreparable rotator cuff tear. *AlloSource White Paper*. 2017; 00125-LIT [003].
8. Williams, R. Acellular dermal grafts augmentation in a quadriceps tendon rupture repair. *Current Orthopaedic Practice*. 2010; 21(3):315–19.
9. Stillwell R, Delaney R. The biomechanics of AlloMend acellular dermal matrix: Biocompatibility study. *AlloSource White Paper*. 2016; 00088-LIT [001].
10. Delaney R, Stillwell R. The biological properties of AlloMend acellular dermal matrix: Growth factor study. *AlloSource White Paper*. 2016; 00104-LIT.
11. Steven PJ, Stilwell R, Castillo L. The biomechanics of AlloMend acellular dermal matrix: Ultimate tensile strength. *AlloSource White Paper*. 2020; 00048-LIT [002].
12. Stilwell R, Delaney R, Castillo L. The biomechanics of AlloMend acellular dermal matrix: Suture retention strength. *AlloSource White Paper*. 2020; 00078-LIT [002].
13. Blume L, Sakthivel R. The biomechanical properties of meshed AlloMend acellular dermal matrix: Fluid egress and surface area. *AlloSource White Paper*. 2019; 00149-LIT [001].
14. Benirschke K, et al. (1978). *Pathology of laboratory animals*. Springer-Verlag.
15. Jubb KVF, et al. (1993). *Pathology of domestic animals*. Academic Press, Inc.
16. Pusztaszeri MP, et al. Immunohistochemical expression of endothelial markers CD31, CD34, von Willebrand factor, and Fli-1 in normal human tissues. *Journal of Histochemistry & Cytochemistry*. 2006; 54(4):385–395.
17. Ching YH, et al. The use of growth factors and other humoral agents to accelerate and enhance burn wound healing. *Eplasty*. 2011; 11: e41.
18. Wang H, et al. Acceleration of skin graft healing by growth factors. *Burns*. 1996; 22(1):10–14.
19. Ching YH, et al.
20. Wang H, et al.
21. Matsumine H. Treatment of skin avulsion injuries with basic fibroblast growth factor. *Plastic and Reconstructive Surgery Global Open*. 2015; 3(4);371.
22. Nissen NN, et al. Basic fibroblast growth factor mediates angiogenic activity in early surgical wounds. *Surgery*. 1996; 119(4):457–65.
23. Akita S, et al. Basic fibroblast growth factor in scarless wound healing. *Advances in Wound Care*. 2013; 2(2):44–49.
24. Zhao S, et al. Biological augmentation of rotator cuff repair using bFGF-loaded electrospun poly(lactide-co-glycolide) fibrous membranes. *Int J Nanomedicine*. 2014; 9(1):2373–85.
25. Ide J, et al. The effect of a local application of fibroblast growth factor-2 on tendon-to-bone remodeling in rats with acute injury and repair of the supraspinatus tendon. *J Shoulder Elbow Surg*. 2009; 18(3):391–8.
26. Ide J, et al. The effects of fibroblast growth factor-2 on rotator cuff reconstruction with acellular dermal matrix grafts. *Arthroscopy*. 2009; 25(6):608–16.
27. Heldin CH, Westermark B. Mechanism of action and in vivo role of platelet-derived growth factor. *Physiological Reviews*. 1999; 79(4):1283–1316.
28. Meyer-Ingold W. Wound therapy: Growth factors as agents to promote healing. *Trends in Biotechnology*. 1993; 11(9):387–92.
29. Pierce GF, et al. Tissue repair processes in healing chronic pressure ulcers treated with recombinant platelet-derived growth factor BB. *The American Journal of Pathology*. 1994; 145(6):1399.

30. Hee CK, et al. Augmentation of a rotator cuff suture repair using rhPDGF-BB and a type I bovine collagen matrix in an ovine model. *Am J Sports Med*. 2011; 39(8):1630-39.

31. Uggen C, et al. The effect of recombinant human platelet-derived growth factor BB-coated sutures on rotator cuff healing in a sheep model. *Arthroscopy*. 2010; 26(11):1456-62.

32. Pakyari M, et al. Critical role of transforming growth factor beta in different phases of wound healing. *Advances in Wound Care*. 2013; 2(5):215-24.

33. Coffey R, et al. Selective inhibition of growth-related gene expression in murine keratinocytes by transforming growth factor beta. *Molecular and Cellular Biology*. 1988; 8(8):3088-93.

34. Penn JW, et al. The role of the TGF-beta family in wound healing, burns and scarring: a review. *Int J Burns Trauma*. 2012; 2(1):18-28.

35. Brown RL, et al. Wound healing in the transforming growth factor beta 1- deficient mouse. *Wound Repair and Regeneration*. 1995; 3(1):25-36.

36. Bedi A, et al. Cytokines in rotator cuff degeneration and repair. *J Shoulder Elbow Surg*. 2012; 21(2):218-27.

37. Manning CN, et al. Sustained delivery of transforming growth factor beta three enhances tendon-to-bone healing in a rat model. *J Orthop Res*. 2011; 29(7):1099-105.

38. Daley SR, et al. A key role for TGF-beta signaling to T cells in the long-term acceptance of allografts. *The Journal of Immunology*. 2007; 179(6):3648-54.

39. Pauly S, et al. BMP-2 and BMP-7 affect human rotator cuff tendon cells in vitro. *J Shoulder Elbow Surg*. 2012; 21(4):464-73.

40. Chen B, et al. Enhancement of tendon-to-bone healing after anterior cruciate ligament reconstruction using bone marrow-derived mesenchymal stem cells genetically modified with bFGF/BMP2. *Sci Rep*. 2016; 6:25940.

41. Chen CH, et al. Enhancement of rotator cuff tendon-bone healing with injectable periosteum progenitor cells-BMP-2 hydrogel in vivo. *Knee Surg Sports Traumatol Arthrosc*. 2011; 19(9):1597-607.

42. Sottile V, Seuwen K. Bone morphogenetic protein-2 stimulates adipogenic differentiation of mesenchymal precursor cells in synergy with BRL 49653 (rosiglitazone). *FEBS Lett*. 2000; 475(3):201-4.

43. U.S. Pharmacopeia 35-NF 30. (2011), 2381. *United States Pharmacopeia.*

44. ASTM International D638-10. (2010), Standard Test Method for Tensile Properties of Plastics, *ASTM International.*

45. Norowski P, et al. Suture pullout strength and in vitro fibroblast and RAW 264.7 monocyte biocompatibility of genipin crosslinked nanofibrous chitosan mats for guided tissue regeneration. *Journal of Biomedical Materials Research, Part A 100.11.* 2012; 2890-96.

46. Mine Y. Suture retention strength of expanded polytetrafluoroethylene (ePTFE) graft. Diss. Okayama University, 2010.

47. Caputo GG, et al. Daily serum collection after acellular dermal matrix-assisted breast reconstruction. *Arch Plast Surg*. 2015; 42:321-26.

48. Brzezinski MA, et al. Classification and management of seromas in immediate breast reconstruction using the tissue expander and acellular dermal matrix technique. *Ann Plast Surg*. 2013; 70:488-492.

6278 S Troy Cir
Centennial, CO 80111
USA

MAIN 720. 873. 0213
TOLL FREE 800. 557. 3587
FAX 720. 873. 0212

allosource.org

00169-LIT[001] - 9/2021